UCLA-ENG--8606

DE86 012880

UCLA-ENG-8606
PPG-932

Thermomechanical Analysis of Solid Breeders in Sphere-Pac, Plate, and Pellet Configurations

James P. Blanchard and Nasr M. Ghoniem

February 1986

This research was performed under appointment to the Magnetic Fusion Energy Technology Fellowship program administered by Oak Ridge Associated Universities for the U.S. Department of Energy. The support of U.S. Department of Energy, Grant #DE-[redacted]03-80ER52061, to UCLA is appreciated.

AS

EAB

CONTENTS

FIGURES

TABLES

1. INTRODUCTION

Fusion blankets featuring solid breeders have been proposed in many different configurations. The "Blanket Comparison and Selection Study" (BCSS) [1], for example, includes breeder-in-tube, breeder-outside-tube, and layered designs. As discussed in the study, each concept has advantages and disadvantages associated with its various components. In this report we will assess the thermomechanical behavior of three common configurations and discuss the implications on blanket design.

The first configuration studied is called sphere-pac. It features small breeder spheres of three different diameters, thus allowing efficient packing and minimal void fraction. The concept originated as an attempt to minimize thermal stresses in the breeder and improve the predictability of the breeder-structure interface heat conduction. It remains a viable option for commercial fusion.

The second concept features plates of solid breeder wrapped with thin steel cladding. The thermal stresses in large plates can reach high levels, so small rectangular blocks will be used in most designs. This shifts much of the load to the cladding, which should be thin for good breeding and thick for good mechanical strength. In general the breeder is made as thin as possible, to maximize the breeding ratio, so the cladding's integrity will likely be the life-limiting issue of this concept.

The third breeder configuration is in the form of pellets cladded by steel tubes. This design is similar to fission fuel rods, but the analysis for fusion differs in two ways:

1. The coolant in fission reactors flows parallel to the fuel rods' axes, whereas fusion designs can be either parallel or cross flow.

2. The flux source in fission reactors is the fuel itself, while in fusion it is the plasma. As a result, the damage gradient over the cross section of a solid breeder pin may be more severe than in fission rods.

The major thermomechanical issue of the pin-type designs is cracking, which would impair the thermal performance of the blanket. Fortunately, the pins can be sized to prevent cracking under normal operation.

In this report we have treated each blanket generically, dealing with basic issues rather than design specifics. Our basic philosophy is to avoid cracking of the breeder if at all possible. It can be argued that cracking could be allowed, but this would sacrifice predictability of the blanket thermal performance and tritium release characteristics. Proper design can and should minimize breeder cracking.

2. SPHERE-PAC BREEDER CONFIGURATION

Because the use of relatively large blocks of solid breeder can lead to severe interaction with the surrounding structure, the sphere-pac concept is an attractive configuration that achieves high net density while reducing the blanket stresses. Three different sphere diameters are used to minimize the voids in the breeder zone. It is assumed, by those who advocate this concept, that the spheres are relatively free to move around as they expand, thus reducing the thermal stresses due to constraint. In this sense, the spheres are believed to act much like a fluid.

Unfortunately, it may not be sufficient to assume that the spheres are unconstrained. One might expect that if the sphere diameter is more than about half of the diameter of the surrounding structure relative motion may be reduced, causing the spheres to act more like a solid. Additionally, sintering could inhibit the idealized behavior of the breeder, leading to cracking or breakage. The following analysis attempts to quantify the possible effects of solid breeder pellet constraint.

2.1. UNCONSTRAINED THERMAL STRESS

Initially we consider the stresses in a free sphere subject to a uniform temperature rise ΔT_b, and uniform volumetric heating q'''. If we assume linear, elastic material behavior and no angular dependence of the temperature, the displacements and stresses are [2]:

$$U = \frac{(1+\nu)}{1-\nu}\frac{\alpha}{r^2}\left[\int_0^r Tr^2 dr + \frac{2(1-2\nu)}{1+\nu}\frac{r^3}{b^3}\int_0^b Tr^2 dr\right] ,$$

$$\sigma_r = \frac{2\alpha E}{1-\nu}\left(\frac{1}{b^3}\int_0^b Tr^2 dr - \frac{1}{r^3}\int_0^r Tr^2 dr\right) ,$$

$$\sigma_\phi = \sigma_\theta = \frac{\alpha E}{1-\nu}\left(\frac{2}{b^3}\int_0^b Tr^2 dr + \frac{1}{r^3}\int_0^r Tr^2 dr - T\right) , \qquad (1)$$

where U is the radial displacement, T is the temperature change from the stress-free state, b is the sphere radius, α is the thermal expansion coefficient, E the Young's modulus, and ν is Poisson's ratio. All material properties are assumed to be homogeneous and independent of temperature. σ_r, σ_θ, and σ_ϕ are the normal stresses in the directions of the spherical coordinates r, θ, and ϕ.

2.1.1. Uniform Temperature Change

For a uniform temperature change, the stresses are zero and the radial displacement at the surface is given by

$$U = b\alpha\Delta T_b \quad . \tag{2}$$

2.1.2. Uniform Volumetric Heating

For a uniform volumetric heating rate q''', the temperature distribution is parabolic [2]:

$$T = \Delta T_b + \frac{q'''}{6k}\left(b^2 - r^2\right) \quad , \tag{3}$$

where k is the thermal conductivity.

Substituting Eq. (3) into the stress and displacement equations (1), we obtain

$$\begin{aligned} \sigma_r &= \frac{\alpha E q'''}{15(1-\nu)k}\left(r^2 - b^2\right) \quad , \\ \sigma_\phi &= \sigma_\vartheta = \frac{\alpha E q'''}{15(1-\nu)k}\left(2r^2 - b^2\right) \quad , \\ U(b) &= b\alpha\left(T_b + \frac{q'''b^2}{15k}\right) \quad . \end{aligned} \tag{4}$$

The stresses are plotted in Fig. 1. The radial stress σ_r is always compressive, while σ_θ and σ_ϕ are compressive near the center (r = 0) and tensile near the surface (r = b). The stress state is equi-triaxial compression near the center and equi-biaxial tension near the surface, so cracking will likely begin at the surface. Surface stresses in Li_2O spheres for various heating rates and sphere radii are given in Table I. As seen, the thermal stresses in an unconstrained 1 mm pellet are quite small, but those in 5 mm pellets exceed

the fracture strength for Li_2O. Complete or partial constraint will only aggravate the potential problems.

2.2. CONSTRAINED THERMAL STRESSES

In some cases, adjoining spheres will not allow free accomodation of thermal expansion. The worst case is one in which the centers of two spheres remain at a fixed distance. This problem is addressed by calculating the change in the distance between centers of two free spheres due to a temperature change and then calculating the force required to restore them to their original position.

Roark [3] gives the stresses and displacements in two identical elastic spheres due to a point load P as

$$\Delta = 1.55\left(\frac{P^2}{E^2 b}\right)^{1/3} , \qquad \sigma_{c,max} = -0.616\left(\frac{PE^2}{b^2}\right)^{1/3} , \tag{5}$$

where Δ is the change in distance between the sphere centers (after free expansion) and $\sigma_{c,max}$ is the maximum compressive stress, which occurs at the contact surface between the two spheres. The maximum tensile stress is about $0.133\ \sigma_{c,max}$ and occurs at the edge of the contact surface.

Setting $\Delta + U(b) = 0$, where $U(b)$ is given by Eq. (4), we obtain

$$P = Eb^2\left[\frac{\alpha}{1.55}\left(T_b + \frac{q'''b^2}{15k}\right)\right]^{3/2} , \tag{6}$$

and the maximum stress is

$$\sigma_{c,max} = -0.616\ E\left[\frac{\alpha}{1.55}\left(T_b + \frac{q'''b^2}{15k}\right)\right]^{1/2} \quad . \tag{7}$$

The stresses given by this formula, ignoring fracture, are in Table I. Obviously, the stresses are very high, but one must consider the model used in this analysis before giving up on the sphere-pac concept.

Sphere-pac was originated to allow accomodation of thermal expansion or swelling, on the premise that relative motion of adjoining spheres would be possible. In general, the constraint of the breeder will be minimized and the resulting stresses will also be small. It is only in certain situations that free expansion is restrained and large stresses are developed. Even then, the constraint will not likely be as severe as those analyzed here. These considerations indicate that a thorough analysis of sphere-pac is difficult and testing is required to verify its feasibility.

3. PLATE CONFIGURATION

One common fusion blanket concept features plates of solid breeder contained by some structural material [1]. The breeders are often quite brittle so thermal stresses can easily lead to cracking in even an unconstrained plate. The cladding, which offers some restraint of the breeder's thermal expansion, compounds the problem. In addition, one would like to minimize the amount of structure in the breeding zone in order to increase the tritium breeding ratio; hence the cladding is generally very thin. In some cases, the cladding may actually be the weakest member of the system. In either case, analysis is needed to assess the integrity of a solid breeder blanket.

To deal with the interaction between breeder plates and their cladding, this report first analyzes the thermal stresses in an unconstrained plate that is essentially infinite in two directions, as seen in Fig. 2. The neutron current is in the z-direction and the temperature varies in both the y- and z-directions, leading to stresses in the z-direction. The impact of the cladding on this stress field is then calculated assuming that it acts like a simple truss member at the top of the plate ($z = 0$). Finally, possible advancements in this analysis are suggested.

3.1. UNCONSTRAINED PLATES

A neutron current in the z-direction, such as that in Fig. 2, will cause a temperature distribution that is independent of x, symmetric about $y = 0$ and which decays exponentially in the z-direction. These conditions imply that the plate will not bend, thus simplifying our analysis. Assuming that there are no stresses in the y-direction because the plate is thin and that there are also none in the x-direction because the uniform heat generation does not vary in that direction, a 1-D analysis is sufficient for the bulk of the plate. We begin with a general equation for the strains in the plate:

$$e^{\tau} = e^{el} + e^{th} + e^{c} + e^{s} \quad , \tag{8}$$

where e^{τ} is the total strain at a point in the breeder, e^{el} is the elastic strain, e^{th} is the thermal strain, e^{c} is the creep strain, and e^{s} is the swelling strain. Assuming linear elastic behavior, e^{el} is given by σ/E, where E is the Young's Modulus. By integrating Eq. (8) over a cross section in the x-y plane, one obtains:

$$\int e^{\tau} dA = \int \frac{\sigma}{E} dA + \int (e^{th} + e^{c} + e^{s}) dA \quad . \tag{9}$$

If E is independent of position, $\int (\sigma/E) dA = F_z/E$ where F_z is the net force on the cross section. This must be zero because there are no applied loads. Additionally, e^{τ} can be taken to be independent of x and y as long as the plate is thin and doesn't bend [4]. Therefore, $\int e^{\tau} dA = e^{\tau} \int dA$, yielding

$$e^{\tau} = \frac{1}{2\ell} \int_{-\ell}^{\ell} (e^{th} + e^{s} + e^{c}) dy \quad , \tag{10}$$

where the integral over x has canceled out.

Substituting Eq. (10) into Eq. (8), the stress is found to be

$$\sigma_z = E(\bar{e}'' - e'') \quad , \tag{11}$$

where

$$e'' = e^{th} + e^{s} + e^{c} \quad ,$$

and

$$\bar{e}'' = \frac{1}{2\ell} \int_{-\ell}^{\ell} e'' dy \quad . \tag{12}$$

The stress is thus determined by the difference between the average and local strains.

3.1.1. Thermal Stresses

In this section, swelling and creep strains are ignored. Assuming that the thermal expansion coefficient α is independent of position and temperature, Eq. (11) becomes

$$\sigma = E\alpha(\bar{T} - T) \quad , \tag{13}$$

where

$$\bar{T} = \frac{1}{2\ell} \int_{-\ell}^{\ell} T dy \quad . \tag{14}$$

Ignoring conduction in the x-z plane, the temperature is given by [5]

$$T = T_c + \frac{q''' \ell^2}{2k} \left[1 - \left(\frac{y}{\ell}\right)^2\right] \quad , \tag{15}$$

where T_c is the coolant temperature, q''' is the uniform volumetric heating rate and k is the breeder thermal conductivity. Integrating over the thickness, one finds

$$\bar{T} = T_c + \frac{q''' \ell^2}{3k} \quad , \tag{16}$$

and

$$\bar{T} - T = -\frac{q''' \ell^2}{2k} \left[\frac{1}{3} - \left(\frac{y}{\ell}\right)^2\right] \quad . \tag{17}$$

This quantity, $(\bar{T} - T)$, depends on z only as q''' depends on z, hence it exhibits an exponential decay due to the decay in the neutron flux.

Substituting Eq. (17) into (13) one obtains

$$\sigma_z = -\frac{E\alpha q''' \ell^2}{2k} \left[\frac{1}{3} - \left(\frac{y}{\ell}\right)^2\right] \quad . \tag{18}$$

For typical reactor conditions, the stresses at $z = 0$ are plotted in Fig. 3. The peak tensile stress is approximately 200 MPa, while the peak compressive stress is -100 MPa. The tensile peak exceeds the fracture stress of the Li_2O, so cracking will occur.

3.1.2. End Effects

Because there are no applied tractions on the breeder surfaces, σ_z must be zero at $z = 0$. Therefore Eq. (13) is only valid some distance away from

the surface. Arguments similar to St. Venant's principle [6] imply that Eq. (13) is valid only for $z > 2\ell$ and σ_z decreases to zero as z approaches zero. Therefore, decreasing the length of the plate or cutting it into small blocks will decrease the stresses, thereby reducing the likelihood of fracture.

This phenonemon was verified using SAP IV, a finite element structural analysis code [7]. As shown in Fig. 4, the stress reaches the value given by Eq. (18) in a distance of about 1.6 ℓ. Therefore blocks of breeder that are less than 3.2 times as long as they are thick will likely have reduced stresses.

3.1.3. Creep Relaxation of Swelling Deformations

If creep and swelling are included in the analysis, the steady-state stresses can either be above or below the initial thermal stresses. In this analysis, we will assume a swelling equation of the form

$$e^s = \frac{1}{3}\frac{\Delta V}{V} = f(T)\ \delta \quad , \tag{19}$$

where δ is the accumulated dose and f(T) gives the temperature dependence. In addition, we will assume

$$\dot{e}^c = A\sigma_z \quad , \tag{20}$$

where A is independent of temperature and $\dot{e}^c$ is the creep strain rate in terms of the dose δ. In other words,

$$e^c = \int_0^{\delta} A\sigma_z d\delta' \quad . \tag{21}$$

Substituting Eq. (21) into Eq. (12), one obtains

$$\bar{e}^c = \frac{1}{2\ell}\int_{-\ell}^{\ell}\int_{0}^{\delta} A\sigma_z d\delta' dy = \frac{A}{2\ell}\int_{0}^{\delta} F_z d\delta' = 0 \quad , \tag{22}$$

where F_z, the applied force, is taken to be *zero for any* cross section. Substituting Eqs. (19), (21), and (22), in Eq. (11), one obtains

$$\sigma_z = \sigma_z^{th} + E\delta[\overline{f(T)} - f(T)] - E\int_{0}^{\delta} A\sigma_z d\delta' \tag{23}$$

where σ_z^{th} is given by Eq. (18) and

$$\overline{f(T)} = \frac{1}{2\ell}\int_{-\ell}^{\ell} f(T)dy \quad . \tag{24}$$

Equation (23) is a first order ODE which is easily solved, giving

$$\sigma_z = \sigma^{th}\exp(-EA\delta) + \frac{\overline{f(T)} - f(T)}{A}[1 - \exp(-EA\delta)] \quad . \tag{25}$$

The initial thermal stress is relaxed exponentially by the creep, while the swelling stresses, which would otherwise increase linearly with dose, are limited to a value determined by the ratio of the swelling and creep rates.

As seen in Eq. (25), stresses in the breeder can become large even if the thermal stresses are tolerable. Unfortunately, the data on the swelling and creep of solid breeder is quite limited, so further analysis will be set aside until these uncertainties are removed.

3.2. *CONSTRAINED PLATES*

The interaction of the solid breeder and its cladding is a complex problem, requiring a 3-D global analysis for a complete description. In order to get a rough estimate of the expected problem, we will assume that the major point of interaction is at the top, $z = 0$, and that the clad and breeder behave as truss members.

Consider two truss members of length 2ℓ that are connected at the ends. The first is made of steel with thickness τ; the second is solid breeder with thickness s. While the breeder is actually quite long, it can be modeled as a truss element with some effective thickness determined by the amount of material which is influenced by the cladding attached to the top.

For the two truss members, we find

$$P_C = K_C(\Delta_C - \Delta_{0C}) \quad ,$$

and

$$P_B = K_B(\Delta_B - \Delta_{0B}) \quad , \tag{26}$$

where P is the load per unit length in the x-direction, K is the stiffness ($K = E\tau/2\ell$), Δ is the total displacement of the end, and Δ_0 is the initial displacement due to thermal expansion.

Because the bars are connected, one requires

$$\Delta_B = \Delta_C \quad ,$$

and

$$P_B + P_C = 0 \quad , \tag{27}$$

where B denotes the breeder and C the cladding. Setting

$$\Delta_0 = 2\ell\alpha T \quad , \tag{28}$$

and solving for P_C yields

$$P_C = \frac{E_C \tau}{1 + (E_C \tau / E_B s)} (\alpha_B - \alpha_C)\bar{T} \quad , \tag{29}$$

where s is the effective thickness of breeder influenced by the cladding. To approximate s, SAP IV was used to analyze a thin truss member attached to the top of a long plate. The stiffness of a 1-cm-thick Li_2O plate was calculated by calculating the load and deflection at the top, due to differential expansion of a 0.25-mm-thick cladding. The breeder stiffness was found to be nearly equal to the cladding stiffness, so

$$\sigma_C = P_C/\tau = \frac{1}{2} E_C(\alpha_B - \alpha_C)\bar{T} \quad . \tag{30}$$

This result will depend on the geometry and materials, but it is adequate for comparison of various configuration options. Stresses predicted by Eq. (30) can be very large because σ_C is proportional to the average temperature rise $\bar{T}$, rather than the gradient $\bar{T} - T$. Therefore, unless $\alpha_B - \alpha_C$ is quite small, the cladding is likely to fracture.

To relieve the stresses due to interaction, a designer may try curving the cladding to allow for expansion. For a semi-circular cladding of radius ℓ, Timoshenko and Goodier [6] determine the stiffness:

$$K_C = \frac{E_C t^3}{6\pi \ell^3} \quad , \tag{31}$$

giving

$$P = \frac{(E_C t/3\pi)\left(\frac{I}{\ell}\right)^2}{1 + \left(\frac{I}{\ell}\right)^2 \frac{E_C \tau}{3\pi E_B s}} (\alpha_B - \alpha_C)\bar{T} \quad . \tag{32}$$

Because the cladding stiffness is reduced by the factor $(1/3\pi)(\tau/\ell)^2$, we can assume $K_C/K_B \ll 1$, giving

$$\sigma_C = P_C/\tau = \frac{1}{3\pi} E_C\left(\frac{\tau}{\ell}\right)^2 (\alpha_B - \alpha_C)\bar{T} \quad . \tag{33}$$

This simple design change has reduced the stress by the factor $(2/3\pi)(\tau/\ell)^2$, which is approximately 0.002 for typical dimensions. Even if bending of this circular cladding is considered, the reduction in stress is significant.

3.3. CONCLUSIONS

The analysis of solid breeder stresses is difficult, complicated by uncertainties in reactor designs, material properties and modeling. The rather simple analyses presented here are nonetheless useful because they provide insight into scaling relationships and possible design changes. They also allow one to consider both swelling and creep, without reverting to complex codes, which can be costly.

It is apparent from this analysis that large solid breeder plates will most likely fracture because of thermal stresses. To avoid such a possibility, small blocks have to be packed into rectangular cladding canisters. However, the flat interaction surfaces of this configuration leads to further problems. It is advisable to contain solid breeders in tubular-type cladding configurations. For typical reactor designs, no analysis will be reliable enough to preclude thorough component testing, so the analysis presented here may suffice until blanket design progresses further.

4. PELLET CONFIGURATION

Because solid breeders are inherently brittle, they are prone to cracking due to thermal gradients, swelling gradients, and external loads or constraint. Since the breeders are not needed to function as structural materials, this cracking is not hazardous, yet it can impede reactor performance. As the breeder pellets crack, their net conductivity and tritium diffusion behaviors change. Additionally, the restructuring and fragmentation can impede purge flow, increasing the tritium inventory. Before cracking is allowed, the designer must understand the pellet behavior under expected operating conditions.

In this section, thermal stresses in solid pellets are calculated for a variety of temperature fields, including azimuthal variations. Because the rods are oriented perpendicular to both the neutron current from the plasma and the coolant flow, the temperature will vary radially and azimuthally. The thermal stresses, therefore, will also be functions of r and θ. Axial stresses will be treated by assuming that the pellets are in a state of plane stress.

4.1. PROBLEM DESCRIPTION

The model chosen for the analysis is seen in Fig. 5. It features a solid cylinder of radius b, with no body forces or surface tractions. The thermal field is assumed to be of the form:

$$T = T_0 - T_{ref} = (T_c - T_{ref}) + T_1\left(\frac{r}{b}\right) f_1(\theta) + \Delta\left(\frac{r}{b}\right)^2 \left[1 + \frac{T_2}{\Delta} f_2(\theta)\right] \quad , \tag{34}$$

where T represents the components of the thermal field that cause stress, T_0 is the operating temperature, and T_{ref} is a zero-stress reference temperature. The thermal field consists of four major components:

1. $T_c - T_{ref}$ is the difference between the operating temperature at the center of the pellet and the reference temperature.

2. $T_1(r/b)f_1(\theta)$ represents an azimuthal variation that is linear in r.

3. $\Delta(r/b)^2$ is obtained when $f_1(\theta) = f_2(\theta) = 0$ and the volumetric heating q''' is constant. In this case,

$$\Delta = -q'''b^2/4k \quad , \tag{35}$$

where k is the thermal conductivity.

4. $T_2(r/b)^2 f_2(\theta)$ represents an azimuthal variation that is quadratic in r.

The functions f_1 and f_2 are general functions of θ which depend upon the flow parameters and neutronics. In this section they will be expanded in a Fourier series and only the first term will be analyzed.

4.2. STRESS ANALYSIS

To simplify the calculations, the four components of the thermal field will be treated separately and the resulting stresses will be superimposed.

4.2.1. Axisymmetric Thermal Field

4.2.1.1. Uniform Temperature. For an axisymmetric thermal field and plane stress conditions, *Olander* [8] gives the following equation for the radial displacement u:

$$\frac{d}{dr}\left[\frac{1}{r}\frac{d}{dr}(ru)\right] = (1+\nu)\frac{d}{dr}(\alpha T) \quad , \tag{36}$$

where ν is Poisson's ratio and α is the coefficient of thermal expansion. Assuming α and ν are independent of r and T, Eq. (36) can be integrated once to yield

$$\frac{d}{dr}(ru) = (1+\nu)\alpha Tr + 2C_2 r \quad , \tag{37}$$

where C_2 is an arbitrary constant.

For constant temperature, Eq. (37) can be integrated to yield

$$u = \left[\frac{1}{2}(1+\nu)\alpha(T_c - T_{ref}) + C_2\right]r + \frac{C_1}{r} \quad . \tag{38}$$

In order to have finite displacement at r = 0, one requires $C_1 = 0$.

To obtain the stress field, one requires stress-strain and strain-displacement equations. Timoshenko and Goodier give the axisymmetric strain-displacement equations [9] as

$$\varepsilon_r = \frac{\partial u}{\partial r} \quad ,$$

$$\varepsilon_\theta = \frac{u}{r} + \frac{1}{r}\frac{\partial v}{\partial \theta} \quad ,$$

$$\gamma_{r\theta} = \frac{1}{r}\frac{\partial u}{\partial \theta} + \frac{\partial v}{\partial r} - \frac{v}{r} \quad , \tag{39}$$

and the plane stress constitutive equations [10] as

$$\sigma_r = \frac{E}{1 - \nu^2} \left[\varepsilon_r + \nu\varepsilon_\theta - (1 + \nu)\alpha T\right] \quad ,$$

$$\sigma_\theta = \frac{E}{1 - \nu^2} \left[\varepsilon_\theta + \nu\varepsilon_r - (1 + \nu)\alpha T\right] \quad ,$$

$$\tau_{r\theta} = G\gamma_{r\theta} \quad . \tag{40}$$

Substituting Eq. (38) into Eq. (39) and then into Eq. (40), one obtains

$$\sigma_r = \sigma_\theta = \frac{E}{1 - \nu} \left[C_2 - \frac{1}{2} (1 - \nu)\alpha(T_c - T_{ref})\right] \quad . \tag{41}$$

Using the boundary condition $\sigma_r(r = b) = 0$, one finds that the pellet is stress free, i.e.,

$$\sigma_r = \sigma_\theta = 0 \quad . \tag{42}$$

Hence, the average pellet temperature has no influence on cracking and only gradients (radial or azimuthal) cause stresses.

The displacement, u, is given by

$$u = \frac{1}{2} \alpha(T_c - T_{ref})r \quad . \tag{43}$$

4.2.1.2. Uniform Volumetric Heating. Starting from Eq. (37), one inserts $T = \Delta(r/b)^2$ and integrates to obtain

$$u = \frac{1}{4} (1 + \nu)\alpha\Delta \frac{r^3}{b^2} + C_2 r + \frac{C_1}{r} \quad . \tag{44}$$

Again, finite displacement requires $C_1 = 0$.

Using Eqs. (39) and (40), the stresses are found to be

$$\sigma_r = \frac{E}{1-\nu^2}\left[(1+\nu)C_2 - \frac{1-\nu^2}{4}\alpha\Delta\left(\frac{r}{b}\right)^2\right] \quad ,$$

$$\sigma_\theta = \frac{E}{1-\nu^2}\left[(1+\nu)C_2 - \frac{3(1-\nu^2)}{4}\alpha\Delta\left(\frac{r}{b}\right)^2\right] \quad . \tag{45}$$

For $\sigma_r(r=b)=0$, $C_2 = (1/4)(1-\nu)\alpha\Delta$, the stresses are

$$\sigma_r = \frac{1}{4}E\alpha\Delta\left[1-\left(\frac{r}{b}\right)^2\right] \quad ,$$

$$\sigma_\theta = \frac{1}{4}E\alpha\Delta\left[1-3\left(\frac{r}{b}\right)^2\right] \quad , \tag{46}$$

and the displacement is

$$u = \frac{1}{4}\alpha\Delta r\left[(1-\nu)+(1+\nu)\left(\frac{r}{b}\right)^2\right] \quad . \tag{47}$$

4.2.2. Non-Axisymmetric Thermal Field

4.2.2.1. $T = T_1(r/b)\cos\theta$. Because of the azimuthal variation introduced here, the previous analysis must be modified. The procedures will involve both stress and displacement potentials, as suggested by Timoshenko and Goodier [11].

To find a particular solution, one introduces a displacement potential ψ, such that

$$u = \psi_{,r} \quad , \qquad v = (1/r)\psi_{,\theta} \quad , \tag{48}$$

where v is the azimuthal displacement and $\psi_{,r}$ represents $\partial\psi/\partial r$. For plane stress, the governing equation for ϕ is

$$\nabla^2\psi = \psi_{,rr} + \frac{1}{r}\psi_{,r} + \frac{1}{r^2}\psi_{,\theta\theta} = (1+\nu)\alpha T \quad . \tag{49}$$

If ψ is expanded in a cosine series, i.e., $\psi = \sum_{n=0}^{\infty} \psi_n \cos n\theta$, then the particular solution will involve only ψ_1 because of the assumed thermal field. Substituting into Eq. (49), one obtains

$$\psi_{1,rr} + \frac{1}{r}\psi_{1,r} - \frac{1}{r^2}\psi_1 = (1+\nu)\alpha T_1\left(\frac{r}{b}\right) \quad . \tag{50}$$

the particular solution to this equation is

$$\psi_1 = -\frac{1}{4}(1+\nu)\alpha T_1 \frac{r}{b}\left(b^2 - \frac{1}{2}r^2\right) \quad , \tag{51}$$

and, from Eq. (48), one finds

$$u = -\frac{1}{4}(1+\nu)\alpha T_1\left(b - \frac{3}{2}\frac{r^2}{b}\right)\cos\theta \quad ,$$

$$v = \frac{1}{4}(1+\nu)\alpha T_1\left(b - \frac{1}{2}\frac{r^2}{b}\right)\sin\theta \quad ,$$

$$\sigma_r = -\frac{1}{4}E\alpha T_1\left(\frac{r}{b}\right)\cos\theta \quad ,$$

$$\sigma_\theta = -\frac{3}{4}E\alpha T_1\left(\frac{r}{b}\right)\cos\theta \quad ,$$

$$\tau_{r\theta} = -\frac{1}{4}E\alpha T_1\left(\frac{r}{b}\right)\sin\theta \quad . \tag{52}$$

Since this is only a particular solution, there are no arbitrary constants that allow us to impose the proper boundary conditions. Therefore, a problem featuring applied surface tractions must be superimposed upon Eq. (52) to yield the proper solution. This problem is best solved using a stress potential ϕ.

The surface tractions required to produce a traction-free surface condition when added to Eq. (52) are

$$\sigma_r(r = b) = \frac{1}{4} E\alpha T_1 \cos\theta \quad ,$$

$$\tau_{r\theta}(r = b) = -\frac{1}{4} E\alpha T_1 \sin\theta \quad . \tag{53}$$

To solve this problem, introduce ϕ such that

$$\sigma_r = \frac{1}{r} \phi_{,r} + \frac{1}{r^2} \phi_{,\theta\theta} \quad ,$$

$$\sigma_\theta = \phi_{,rr} \quad ,$$

$$\tau_{r\theta} = -\frac{\partial}{\partial r} \left(\frac{1}{r} \phi_{,\theta}\right) \quad . \tag{54}$$

The governing equation is

$$\left(\frac{\partial^2}{\partial r^2} + \frac{1}{r}\frac{\partial}{\partial r} + \frac{1}{r^2}\frac{\partial^2}{\partial \theta^2}\right)\left(\phi_{,rr} + \frac{1}{r} \phi_{,r} + \frac{1}{r^2} \phi_{,\theta\theta}\right) = 0 \quad , \tag{55}$$

and the solution is $\phi = Ar^3 \cos\theta$, where A is an arbitrary constant. This leads to

$$\sigma_r = 2Ar \cos\theta \quad ,$$

$$\sigma_\theta = 6Ar \cos\theta \quad ,$$

$$\tau_{r\theta} = 2Ar \sin\theta \quad . \tag{56}$$

Using Eq. (53) one finds $A = (1/8b)E\alpha T_1$ and

$$\sigma_r = \frac{1}{4} E\alpha T_1 \left(\frac{r}{b}\right) \cos\theta \quad ,$$

$$\sigma_\theta = \frac{3}{4} E\alpha T_1 \left(\frac{r}{b}\right) \cos\theta \quad ,$$

$$\tau_{r\theta} = \frac{1}{4} E\alpha T_1 \left(\frac{r}{b}\right) \sin\theta \quad . \tag{57}$$

Adding Eqs. (57) and (52) to obtain the total solution, one again finds that the pellet is stress-free. This is not surprising if one considers the nature of the assumed thermal field. When $T = \Delta(r/b)\cos\theta$, the contours of constant temperature are straight lines perpendicular to the coolant flow. In other words, T varies linearly with distance from the plasma. This, intuitively, is a zero-stress situation.

4.2.2.2. $T = T_2(r/b)^2 \cos\theta$. In this case, the particular solution to Eq. (49) is

$$\psi = -\frac{1}{6} (1 + \nu) \alpha T_2 r \left(b - \frac{2r^3}{5b^2}\right) \cos\theta \quad , \tag{58}$$

and the stresses are

$$\sigma_r = -\frac{1}{5} E\alpha T_2 \left(\frac{r}{b}\right)^2 \cos\theta \quad ,$$

$$\sigma_\theta = -\frac{4}{5} E\alpha T_2 \left(\frac{r}{b}\right)^2 \cos\theta \quad ,$$

$$\tau_{r\theta} = -\frac{1}{5} E\alpha T_2 \left(\frac{r}{b}\right)^2 \sin\theta \quad . \tag{59}$$

To obtain a traction-free surface, one solves Eq. (55) for

$$\sigma_r(r = b) = \frac{1}{5} E\alpha T_1 \cos\theta \quad ,$$

$$\tau_{r\theta}(r = b) = \frac{1}{5} E\alpha T_1 \sin\theta \quad , \tag{60}$$

and adds the result [from Eq. (56)] to Eq. (59) to obtain the final solution:

$$\sigma_r = \frac{1}{5} E\alpha T_2 \left(\frac{r}{b}\right)\left(1 - \frac{r}{b}\right)\cos\theta \quad ,$$

$$\sigma_\theta = \frac{3}{5} E\alpha T_2 \left(\frac{r}{b}\right)\left(1 - \frac{4}{3}\frac{r}{b}\right)\cos\theta \quad ,$$

$$\tau_{r\theta} = \frac{1}{5} E\alpha T_2 \left(\frac{r}{b}\right)\left(1 - \frac{r}{b}\right)\sin\theta \quad . \tag{61}$$

4.3. RESULTS

Using the material parameters in Table II, stresses are tabulated in Table III for various reactor parameters and pellet dimensions. In all cases the stress given is the hoop stress σ_θ at the surface, which is the maximum tensile stress in the pellet.

For typical parameters of a 1-cm-diam pellet and 50-MW/m^3-volumetric heating, the peak tensile stress for $T_2 = 0$ is 215.6 MPa, well above the fracture strength of the pellet. To just avoid the cracking that would result from uniform heating, the pellet radius would have to be changed to 6.5, 3.75, and 2.9 mm for heating rates of 10, 30, and 50 MW/m^3, respectively.

The effect of azimuthal temperature variation is seen in the last column of Table III. Even for $T_2 = 20°C$, which would represent a difference of 40°C

between the front and back of the pellet, the stresses are only 11 MPa. For pellets with diameters on the order of 1 to 2 cm, T_2 should be much less than 20°C and the corresponding stresses should be quite small. This indicates that the nonsymmetric effects are relatively unimportant, so axisymmetric thermal fields could be used in a complex, nonlinear inelastic analysis without sacrificing the integrity of the solution.

4.4. CONCLUSIONS

According to the calculations presented here, cracking of solid breeder pellets can be avoided by the proper choice of their radii. This optimal pellet size is reasonable when thermal stresses are considered. Other factors not discussed are stresses due to the interaction of irradiation creep and swelling. The equally important problem of breeder-cladding interaction is discussed elsewhere in the report.

Another significant result of this work is the relatively small effect of azimuthal variations in the thermal field. This indicates that further analysis can be carried out assuming axisymmetric behavior.

ACKNOWLEDGMENTS

This research was performed under appointment to the Magnetic Fusion Energy Technology Fellowship program administered by Oak Ridge Associated Universities for the U. S. Department of Energy. The support of Department of Energy, Contract DE-FG03-80ER52061 to UCLA is appreciated.

REFERENCES

1. M. A. Abdou et al., "Blanket Comparison and Selection Study," Argonne National Laboratory Report ANL/FPP-84-1, 1984.
2. Franklin Institute Research Laboratories, Thermal Stress Techniques in the Nuclear Industry, (American Elsevier, New York, 1985).
3. R. J. Roark, Formulas for Stress and Strain, (McGraw-Hill, New York, 1975) p. 516.
4. T. H. Lin, Theory of Inelastic Stresses, (Wiley & Sons, New York, 1968) p. 128.
5. A. J. Chapman, Heat Transfer, (Macmillan, New York, 1967) p. 55.
6. S. P. Timoshenko and J. N. Goodier, Theory of Elasticity, (McGraw-Hill, New York (1934) p. 39.
7. K. Bathe et al., "SAP IV, a Structural Analysis Program for Static and Dynamic Response of Linear Systems," Earthquake Engineering Research Center Report EEC 73-11 (1974).
8. D. R. Olander, Fundamental Aspects of Nuclear Reactor Fuel Elements, U.S. Energy Research and Development Office, NTIS TID 26711-P1 (Nat. Tech. Info. Serv., Springfield, VA, 1976) p. 574.
9. S. P. Timoshenko and J. N. Goodier, op. cit., p. 76.
10. Ibid., p. 442.
11. Ibid., p. 481.

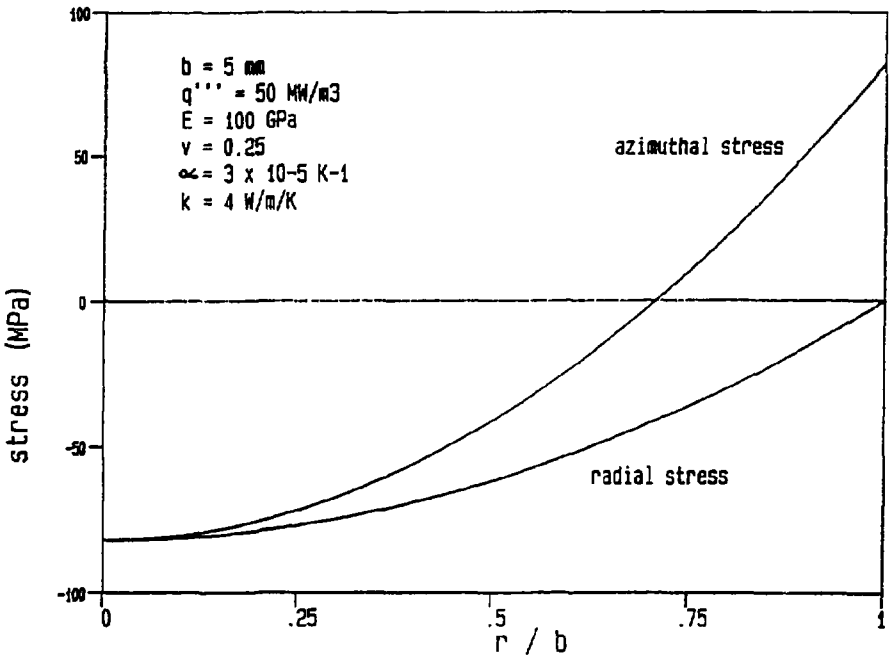

Fig. 1. Thermal stresses in an unconstrained sphere subjected to uniform volumetric heating.

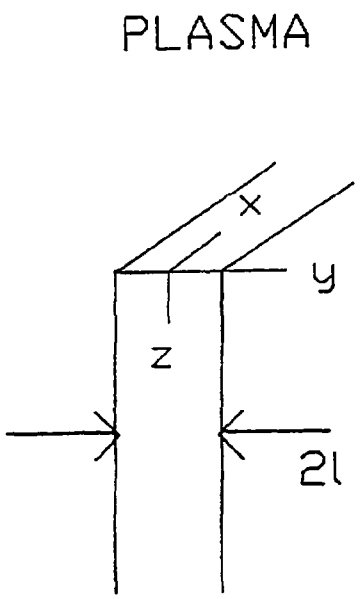

Fig. 2. Model used for breeder plate analysis.

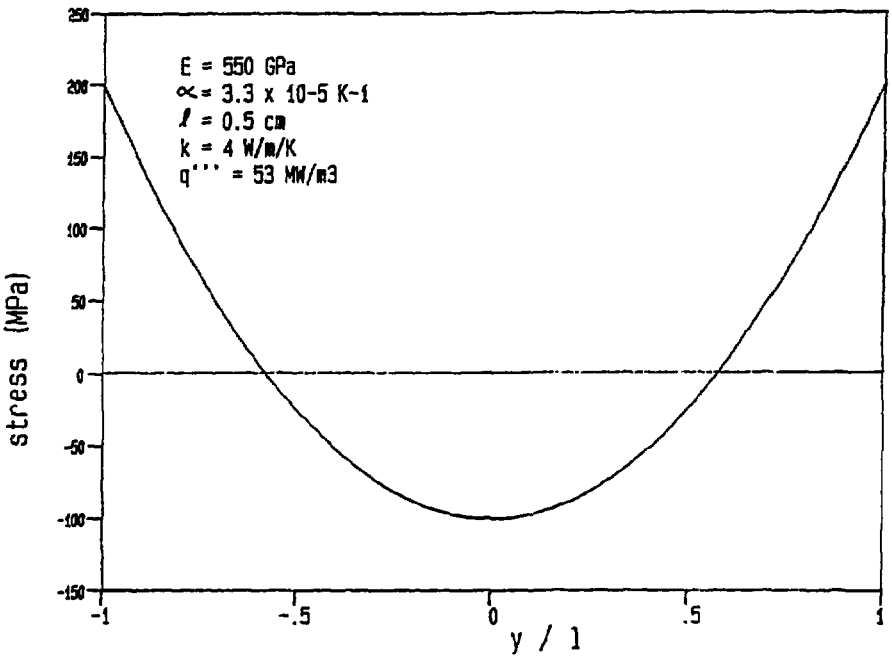

Fig. 3. Axial stresses near top of plate subjected to neutron flux

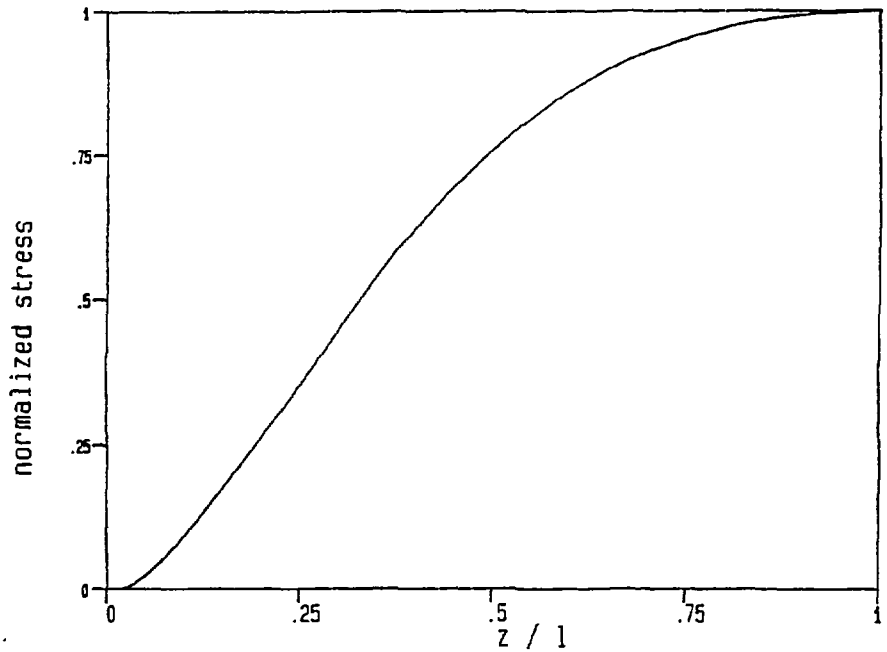

Fig. 4. Effect of free surface on the axial stress distribution at the top of the plate.

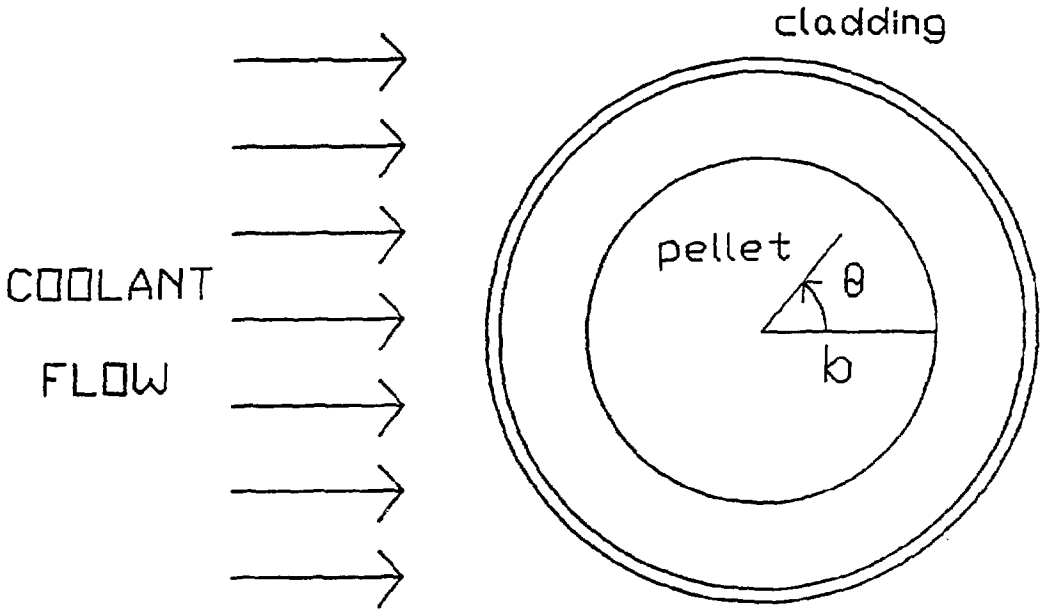

Fig. 5. Model used for breeder pellet analysis.

TABLE I

MAXIMUM STRESSES IN BREEDER SPHERES

b (mm)	q''' (MW/m^3)	ΔT_b (K)	σ (unconstrained) (MPa)	σ (constrained) (MPa)
1	50	600	3.3	7000
1	50	0	3.3	260
1	10	0	0.7	120
5	50	0	82.0	1300

TABLE II

$LiAlO_2$ PROPERTIES

$E = 230 \times 10^3$ MPa

$\alpha = 1.2 \times 10^{-5}\ C^{-1}$

$\nu = 0.23$

$k = 2$ W/mk

$\sigma_{fracture} = 72.8$ MPa (tensile)

TABLE III

MAXIMUM TENSILE STRESSES IN SOLID BREEDER PELLETS

b (mm)	q''' (MW/m^3)	T_2 (°C)	$\sigma_{axysymmetric}$ [(a)] (MPa)	$\sigma_{nonsymmetric}$ [(b)] (MPa)
5	50	-20	215.6	11.0
2.9	50	0	72.8	0
3.75	30	0	72.8	0
6.5	10	0	72.8	0
5	10	-20	43.1	11.0
5	10	-10	43.1	5.5

(a) $T_2 = 0$

(b) $q''' = 0$